Desalination and Water Treatment
www.deswater.com

doi: 10.5004/dwt.2020.25602

189 (2020) 264–275
June

Synthesis and characterization of recyclable O-carboxymethyl chitosan Schiff base for the effective removal of Cd(II) from aqueous solution

Weili Wang[a,*], Qi Lu[b], Zihan Zhuo[a], Wenhui Zhang[a], Haiwen Liu[a], Jiming Zhang[b,*], Jianhua Zhou[b], Yuzhong Niu[a], Tomás Guerrero[c]

[a]*School of Chemistry and Material Science, Ludong University, Yantai, 264025, China, Tel. +86 535 6672609; Fax: +86 535 6696162; emails: wangweilishou@163.com (W. Wang), 2233491128@qq.com (Z. Zhuo), vea2007@126.com (W. Zhang), 15684193510@163.com (H. Liu), niuyuzhong@126.com (Y. Niu)*
[b]*School of Chemistry and Pharmaceutical Engineering, Qilu University of Technology, Jinan 250353, P.R. China, Tel. +86 531 89631208; emails: jmzhang@yeah.net (J. Zhang), 13583158861@163.com (Q. Lu), zhoujianhua4@163.com (J. Zhou)*
[c]*Instituto de Ciencias Básicas-Universidad Veracruzana, Av. Dr. Luis Castelazo Ayala s/n, Col. Industrial Ánimas, Xalapa, Veracruz, C.P. 91190, Mexico, email: tguerrero@uv.mx (T. Guerrero)*

Received 24 May 2019; Accepted 3 February 2020

ABSTRACT

A novel O-carboxymethyl chitosan Schiff base (OCMCS-SB) was synthesized by condensation of O-carboxymethyl chitosan and o-vanillin and evaluated as an adsorbent for Cd(II). The structure of the chitosan Schiff base was characterized through Fourier transform infrared spectroscopy, thermogravimetric analysis/differential thermal gravity, X-ray diffraction and scanning electron microscopy. The effect of adsorbent dose, pH, concentration, the contact time was evaluated in the adsorption experiments of Cd(II). The optimum adsorption pH value was found at 5.5. The adsorption isothermal data fitted well with the Langmuir isotherm equation, the kinetics of adsorption was best described by a pseudo-second-order model. The maximum adsorption is gained at 480 min as 46.72 mg/g and after that the adsorption attained equilibrium. This OCMCS-SB results to be an excellent adsorbent with good selectivity for Cd(II) from a multi-ionic system, was successfully recycled for several runs without significant loss in its adsorption activity.

Keywords: Carboxymethyl chitosan; Schiff base; Adsorption; Cd(II); Recycle

1. Introduction

Environmental pollution with heavy metal ions has become one of the serious environmental threats [1], among them, lead, cadmium, mercury, among others are particularly toxic, all are nonbiodegradable and difficult to separate from wastewater, threatening human health and destroying the ecosystem [2,3]. Within this context, the removal of Cd(II) is considered crucial. Several methods have been developed to remove metal ions, such as chemical precipitation [4], membrane filtration [5] and adsorption [6–8]. Due to their low cost, easy availability and efficiency [9,10], adsorption techniques have attracted the attention of the scientific community. Different kinds of functional materials have been synthesized and used as adsorbents to remove metal ions from aqueous solution [11,12] or organic solvents [13,14], such as dendrimers [15,16], magnetic polymers [17,18], polyfibers [19], silica gel composites [20] and nanomaterials [21,22]. Besides good adsorption ability, most of these adsorbents could be recycled easily due to very stable structures in solution.

Among the above-mentioned materials, natural biopolymers have become very popular, especially because biopolymers are considered low cost, high availability and easily synthesized materials also are environmentally friendly and

* Corresponding authors.

biocompatible and biodegradable [23]. For instance, cross-linked starch phosphates were used for Zn(II) adsorption [10], buckwheat hulls were used for biosorption of Hg(II) [24], organotriphosphonic acid-functionalized japonica shells were applied in the uptake of gold ions [25], acid-treated tea waste was applied for adsorptive removal of Cu^{2+} and direct sky blue 5B from aqueous [26], among others.

As an emergent biopolymer, chitosan is essentially a D-glucosamine based polysaccharide and is one of the most abundant natural polymers on earth after cellulose [27–29]. The physicochemical properties of this biopolymer and above-mentioned applications have to make chitosan emerge as a very attractive biopolymer for materials design, especially in biomedical, agricultural and environmental fields [30–32]. However, the use of chitosan is limited by its poor solubility in water. The free amine groups within the structure of chitosan make possible further chemical modifications [33,34], resulting in interesting derivatives, for instance, chitosan hybrid composite films were developed to remove Hg(II) ions [35]. Adsorption behaviors of chitosan functionalized by amino-terminated hyperbranched polyamidoamine were studied towards Hg (II) adsorption [36]. Chitosan-coated cotton fibers were applied for removal and recovery of Hg(II) from aqueous solution [37] and in our previous work [38], a polymeric ECH cross-linked chitosan Schiff base-sodium alginate was prepared and used as an adsorbent to remove toxic Cd(II) ion from aqueous solution, all these indicating that the modified chitosans have the potential capability to remove metal ions.

On another hand, Schiff bases which provide an imine (–N=CH–) functional group in the molecule, which is known to act as a ligand in coordination chemistry [39–42] and are easily obtained by the condensation of amines with aldehydes or ketones. The amine group can be used to functionalize the chitosan C-2 position in reactions or with metal ions for complexation properties of biopolymer yielding a material with the environmental application [43]. The adsorbents with Schiff bases have been reported elsewhere with excellent results [18,44,45]. Furthermore, these adsorbents are thermally stable and over a wide range of pH without hydrolyzing and can be recycled several times. In this paper, our work aims to synthesis the novel O-carboxymethyl chitosan Schiff base (OCMCS-SB) from O-carboxymethyl chitosan (OCMCS) and o-vanillin using as an adsorbent for efficient adsorption of Cd(II) ion.

2. Experimental

2.1. Materials

Chitosan was purchased from Sinopharm Chemical Reagent Co., Ltd. China, with a weight-average molecular weight (M_w) of 4.6×10^5 and a deacetylation degree (DD) of 90%. Sodium hydroxide, monochloroacetic acid, methanol, ethanol, isopropanol, $Cd(CH_3COO)_2$, o-vanillin were of analytical grade from commercial sources.

2.2. Characterization

Infrared spectra were recorded on an IR Prestige-21 Fourier transform infrared (FTIR) spectrophotometer (KBr). Scanning electron microscopy (SEM) images were taken on FEI Quanta 200 field-emission SEM. X-ray diffraction (XRD) patterns were recorded on a Bruker D8 advance diffractometer using Cu Kα radiation (λ = 1.5406 Å) with a step size of 0.3° 2θ s^{-1}, operating at 40 kV and 40 mA. The thermogravimetric analysis was conducted using a Q600 simultaneous DSC-TGA. The TG/DTA curves were carried out under a nitrogen atmosphere and at a sample heating rate of 10°C min^{-1}.

2.3. Synthesis of OCMCS

OCMCS was obtained by already published protocols as described by Chen and Park [46]. 0.5 g of chitosan was dissolved in isopropanol (20 mL) and stirred for 20 min. 1.0 g (25 mmol) of sodium hydroxide in distilled water (20 mL) was added dropwise under continuous stirring for 1 h at room temperature. After the elapsed time, the mixture was heated at 60°C, and at this temperature, 0.7 g (7.41 mmol) of chloroacetic acid dissolved in isopropanol (10 mL) was added dropwise to the above solution and stirred for another 3 h. The reaction mixture was dissolved in distilled water, and then neutralized by diluted acetic acid. Then, the unreacted chitosan was removed by filtration. The water-soluble portion was precipitated by ethanol, filtrated, and washed with ethanol. The white OCMCS solid was dried in a vacuum oven at 50°C for 6 h (Fig. 1).

2.4. Synthesis of OCMCS-SB

The OCMCS (0.2 g) was swelled in 20 mL of methanol at room temperature for 1 h. Then, a solution of 0.3 g (1.97 mmol) of o-vanillin in 10 mL of methanol was slowly added into the mixture under stirring. This reaction was stirred under reflux temperature for 4 h. After elapsed time, the product was filtrated, washed with methanol and extracted with a Soxhlet flask with ethanol, and then dried in a vacuum oven at 50°C for 6 h, the OCMCS-SB was obtained as a white solid (Fig. 1).

2.5. Adsorption experiment of Cd(II)

A series of adsorption experiments were performed to evaluate the adsorption capacities of OCMCS-SB, OCMCS, and chitosan. Adsorption experiments were controlled by varying pH value, initial Cd(II) concentration, and contact time under the aspects of adsorption isotherms and adsorption kinetics. For the pH effect experiments, 40 mL (40 mg/L, pH = 2–6) of Cd(II) solution was added to conical flasks, the pH of the solution was adjusted with HCl (0.1 mol/L) or NaOH (0.1 mol/L) to attain 2–6, and then 20 mg OCMCS-SB was added. To understand the effect of temperature on adsorption, experiments were carried out at temperatures ranging from 25°C to 45°C. The mixed solution was stirred at 50~200 rpm/min for 4 h, the stirring speed as 100 rpm/min was found to be the proper one. For the adsorption isotherms experiments, 40 mL of Cd(II) solutions (concentration from 15 to 200 mg/L) with 20 mg OCMCS-SB was added to the conical flasks, the pH values of the solution was adjusted to 5.5. Then the mixture was stirred with a speed of 100 rpm/min at 30°C for 10 h. For the adsorption kinetics experiments, 40 mL (100 mg/L) of Cd(II) solution and 20 mg OCMCS-SB was added to the conical flasks, pH was adjusted to 5.5 and stirred with the speed of 100 rpm/min at 30°C for 10 h. The

end solutions through filtration after adsorption were measured by inductively coupled plasma optical emission spectrometry (ICP-MS). The adsorption (Q_e) was defined as the following Eq. (1) [47]:

$$Q_e = \frac{V\left(C_0 - C_e\right)}{M} \quad (1)$$

where Q_e (mg/g) is the amount of Cd(II) adsorbed, V (L) is the volume of the solution, C_0 (mg/L) and C_e (mg/L) are the initial and final concentrations of Cd(II), M (g) is the mass of adsorbent.

Adsorption selectivity of OCMCS-SB was tested under competitive conditions. About 20 mg of the OCMCS-SB was contacted with a binary mixture system, in which the concentration of each metal ion was equal (0.4 mmol/L). The mixture was stirred with 100 rpm/min at 25°C for 24 h. The selectivity was defined as the ratio of adsorption capacities of the two metal ions in the binary mixture.

2.6. Experiments of recycling and reuse of OCMCS-SB

After the adsorption experiments, the Cd(II) adsorbed OCMCS materials were regenerated with desorption with EDTA, 0.1 M HCl, and deionized water until the eluent pH was 7.0. Then the OCMCS-SB was dried at 40°C and used for further adsorption experiments. For Cd(II) recovery, 20 mg of the OCMCS-SB with adsorbed metal ions were placed on a funnel, and 20 mL of diluted hydrochloric acid was used to flush them three times, washed with 80 mL deionized water, and the concentration of Cd(II) in the filtrate was determined via ICP-MS.

3. Results and discussion

3.1. Characterization of the adsorbent

3.1.1. IR data analysis

FTIR was employed to characterize the chitosan (a), OCMCS (b) and OCMCS-SB (c) in Fig. 2. As shown in Fig. 2a shows the characteristics of chitosan at 3,381 cm^{-1} (O–H stretch), 2,873 cm^{-1} (C–H stretch), 1,664 cm^{-1} (amide I bend), 1,593 cm^{-1} (N–H bend), 1,155 cm^{-1} (bridge–o stretch) and 1,082 cm^{-1} (C–O stretch), which agree with already published data [48]. Compared with chitosan, OCMCS (Fig. 2b) has the expected band around 1,411 cm^{-1}, which is attributed to the symmetrical stretching vibration of the COO^- group [49]. A broad peak appears around 1,598 cm^{-1}, which resulted from the asymmetric stretching of –C=O [50]. The C–O absorption peak of the secondary hydroxyl group became stronger and was converted to 1,072 cm^{-1} and indicated the carboxymethyl groups to be on the –OH position. For OCMCS-SB (Fig. 2c), the absorption bands at 1,625 cm^{-1} (–C=N–), 838 cm^{-1} (phenyl) and at 1,250 cm^{-1} (–OCH_3) showed the presence of OCMCS-SB.

3.1.2. Thermal behavior

The thermal stability of chitosan and chitosan derivatives was evaluated by thermogravimetric analysis. As shown in the TG and DTG curves of chitosan in Fig. 3a, for the first stage (r.t. ~ 130°C) a weight loss of 7.57%, was related to the loss of physically adsorbed water molecules. In a second stage (200°C–456°C) a weight loss of 53.53% reaches a maximum at 298°C, which was attributed to the decomposition of chitin and chitosan polymer. In the last stage (456°C–1,000°C) a weight loss of 10.39%, which belonged to the decomposition of the glucosamine residual. The TG and DTG graphs of OCMCS were shown in Fig. 3b, three mass loss stages in the course of thermal decomposition are easily observed.

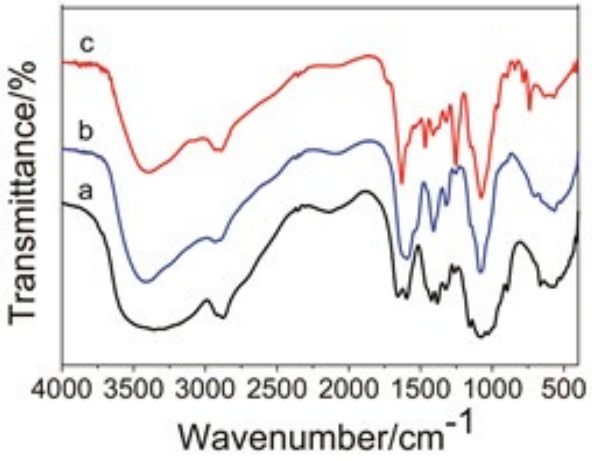

Fig. 2. IR-Spectra of chitosan (a), OCMCS (b), OCMCS-SB, and (c) adsorption.

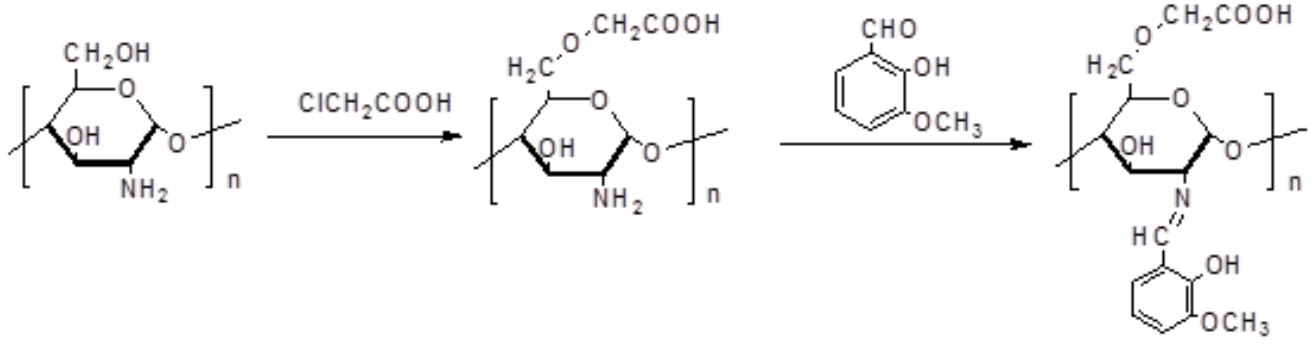

Fig. 1. Synthesis of O-carboxymethyl chitosan Schiff base (OCMC-SB).

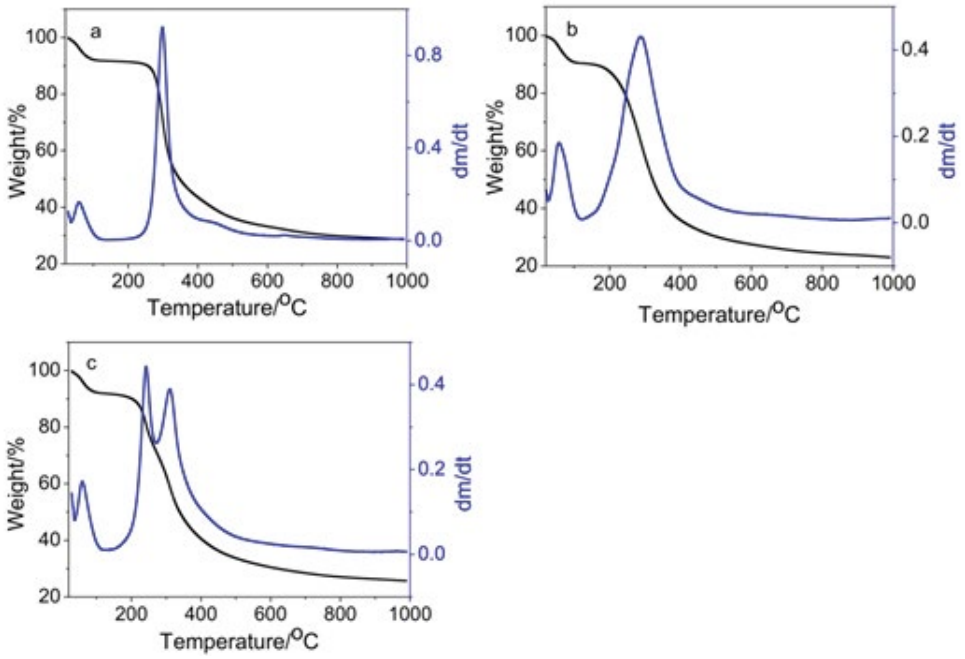

Fig. 3. (a) TG/DTG curves of chitosan, (b) OCMCS, and (c) OCMCS-SB.

The first weight loss (9.55%) at r.t. ~ 97°C was attributed to the loss of surface water molecules. The second stage with a weight loss of 55.15% at 97°C–410°C, was attributed to the thermal decomposition of CMCS unit and the last stage with a weight loss of 13.3% at 410°C–1,000°C may be attributed to the decay of condensed chitosan unit. Fig. 3c displays the TG and DTG curves of OCMCS-SB. In the first stage (below 100°C) a weight loss of 7.87%, which because of the loss of surface water. In the second stage (110°C–470°C) with a weight loss of 57.18%, this refers to the decomposition of the OCMCS-SB unit. The last stage (470°C–1,000°C) with a mass loss of 9.4%, it was due to the decay of the condensed chitosan unit. The two peaks in DTG for OCMCS-SB compound in the range 110°C–470°C refer to the loss of o-vanillin and O-carboxymethyl groups.

3.1.3. XRD analysis

The XRD patterns of chitosan (a), OCMCS (b) and OCMCS-SB (c) were shown in Fig. 4. The significant diffraction peak appeared at a 2θ angle of 20°. For the XRD patterns of OCMCS, OCMCS-SB, apparently, the strength of the peak at a 2θ angle of 22° weakened and was difficult to observe. This can be interpreted as the reduction in the number of amino groups and destroying the intermolecular hydrogen bonds, which resulted in a decrease in the crystallinity of the polymer.

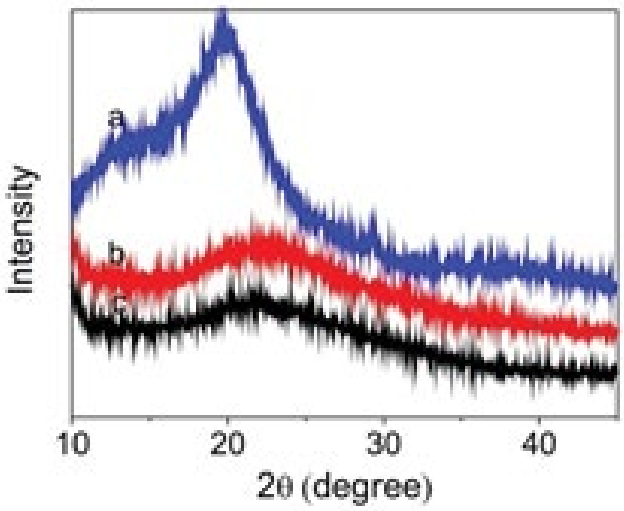

Fig. 4. (a) XRD patterns of chitosan, (b) OCMCS, and (c) OCMCS-SB.

3.1.4. SEM analysis

It exhibits the SEM photos of chitosan (a), OCMCS (b) and OCMCS-SB (c) in Fig. 5. The surface morphology of chitosan, as shown in Fig. 5a revealed its fibrous and flaky properties [51]. From Figs. 5b and c, definitely some structural differences within the surface are observed. These clear changes provided additional proof for two steps of modified chitosan. It showed the heterogeneous pores from the surface of OCMCS-SB which is the predominant cause for adsorption.

3.2. Adsorption of Cd(II) on OCMCS-SB

3.2.1. Effect of adsorbent dose

The adsorbent dose is the main affecting factor in the adsorption process and the potential capacity of the

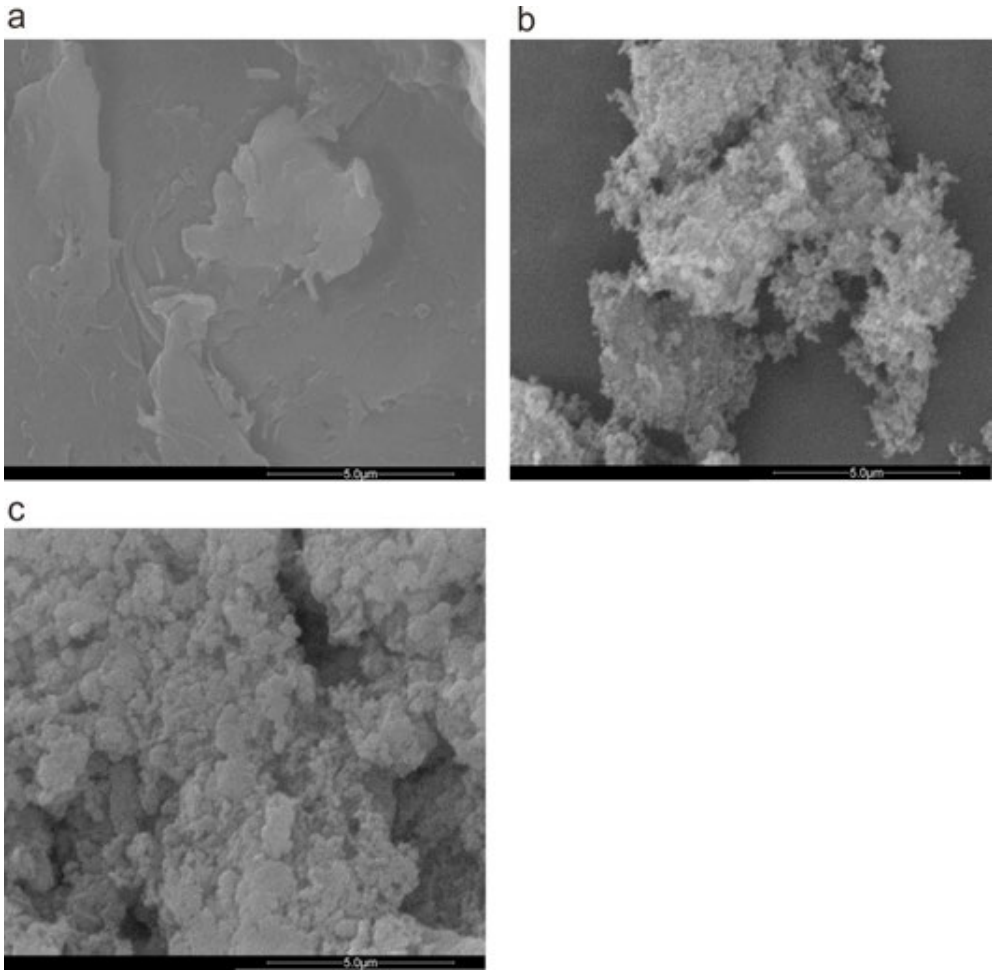

Fig. 5. (a) SEM images of chitosan, (b) OCMCS, and (c) OCMCS-SB.

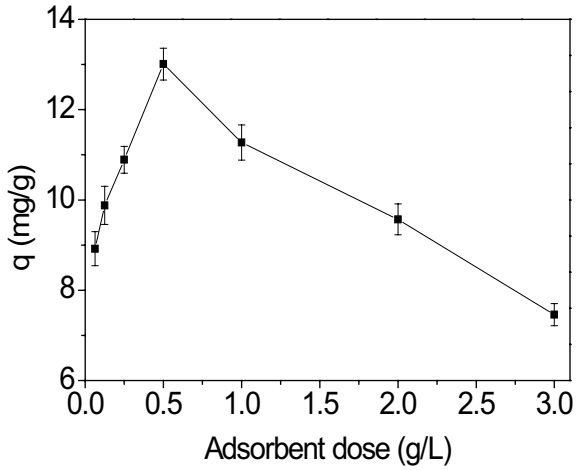

Fig. 6. Effect of adsorbent dose on sorption of Cd(II).

adsorbent. It depends on the effective binding sites to capture heavy metal ions from certain initial concentrations. At equilibrium in Fig. 6, the Cd(II) ion adsorption capacity increases with the increase of adsorbent dose from 0.01 to 0.16 g/L, due to enough available adsorption sites on the adsorbent. However, it decreases while the adsorbent doses > 0.16 g/L. There is no corresponding increase in adsorption resulting from the lower adsorptive capacity utilization of the adsorbent [52]. Therefore, 0.16 g/L of adsorbent was chosen as the optimal dose for further experiments.

3.2.2. Effect of pH

It is known that pH affects the adsorption process deeply [53]. As showed in Fig. 7a, the saturated adsorption capacity of Cd(II) increases with a markedly increase of solution pH values from 2 to 5.5, because the competition between H_3O^+ ion and heavy metal ion decreased. The precipitate of Cd(II) hydroxide would occur beyond pH 5.5, then decreased the concentration of the free heavy metal ions, thereby the sorption capacity of metal ions was declined, so the pH 5.5 was selected as the best pH value for the experiments.

This trend could be rationalized with the surface charge of adsorbent and pH_{pzc}. At $pH < pH_{pzc}$, electrostatic repulsion results in a dominant species with a high positive charge density that hinders the adsorption of Cd(II) ions. While $pH > pH_{pzc}$, the surface of the adsorbent is negatively charged,

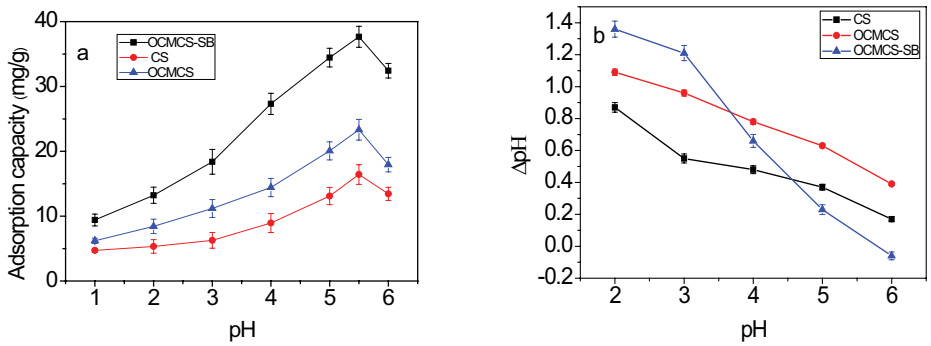

Fig. 7. (a) Effect of pH value on adsorption capacity of Cd(II) and (b) solution pH change before and after the addition of adsorbents.

the enhancing electrostatic attraction would raise the metal ions adsorption [54].

The variation of pH before and after the addition of adsorbent in Fig. 7b proved that the adsorbent surface protonation and deprotonation process occurred during the adsorption process [55]. To get further insight in the influence of pH in the absorption process it is necessary to point out some considerations about the speciation of the carboxylate moiety within the whole range of pH (0–14), the imine group, which is known to be highly sensitive to get hydrolyzed in acidic media and the speciation of cadmium during the absorption process. Concerning the carboxylic acid, it is normally accepted that pKa's are commonly found in a range between 3.745 and 4.869 [56], therefore in the water at pH = 5.5, it is expected that this functional group behaves as a carboxylate moiety, which is expected to act in some extent as a coordinating ligand, nevertheless low coordination ability is also expected as a monodentate ligand, instead, it is known by Quantum Theory of Atoms in Molecules (QTAIM) analysis-that pyranose oxygen atom could act as an electronic density donor [57] allowing a tridentate chelate structure to occur in this range of pH. Concerning the formation of the imine, it is well documented the chemical nature of the imine group [58] also, the hydrolysis of imine functional group in aqueous media is known to occur at pH below six, nevertheless the presence of the aromatic ring of the initial aldehyde and the occurrence of a known template guided reaction [59] suggests the possibility of a highly stable chelate compound which enhances the robustness of the complex even at a slightly acidic media, is important to recall that we don't expect to work in very acid solutions since the main goal is to achieve remediation of anthropogenic polluted waters in which pH values are normally not so acid. Concerning cadmium (II) speciation, the stability constants of cadmium (II) ion are reported elsewhere [60], hence it is described the existence of four hydroxyl complexes of cadmium, the solubility constant of the insoluble $Cd(OH)_2$ complex is also available. From reported constants, it was possible to approximate the corresponding pKa values of acid-base pairs of cadmium (II) hydroxyl complexes and it was estimated that until approximately pH = 9, the concentration of a complex of the type $Cd(OH)_2$ where the corresponding precipitate would appear is negligible, therefore at a pH between the range of 5–8 cadmium(II) will be in ionic form, in such a way that could be adsorbed by the modified chitosan compound. To the best

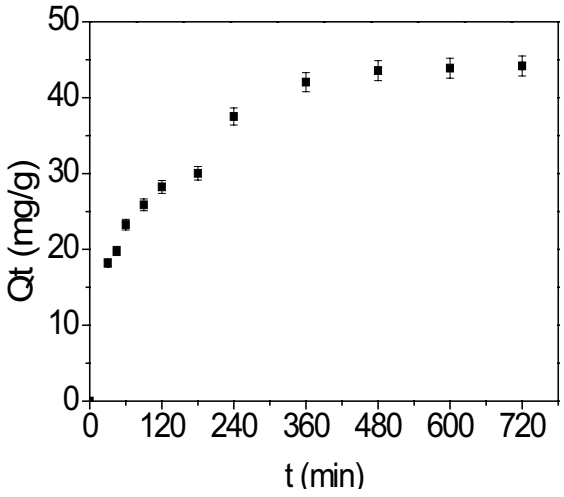

Fig. 8. Effect of contact time on adsorption capacity of Cd(II).

of our knowledge, there are no reported stability constants of this kind of complexes, nevertheless, with this results and already published data, we support that the introduction of o-vanillin and O-carboxymethyl groups into the structure of chitosan provided two structural templates that enhance the adsorption of cadmium (II) by this material.

3.2.3. *Effect of contact time*

In Fig. 8, it illustrates the effect of contact time of Cd(II) on the adsorption capacity by OCMCS-SB. The adsorption capacity increased with increasing contact time. The maximum adsorption is gained in 480 min and after that the adsorption attained equilibrium. The contact time of 480 was regarded as enough to achieve saturation. This can be explained that the adsorption sites were free and that the adsorbate easily interacted with these sites at the initial stage. With time increasing, the remaining void sites were not easily absorbed, until they reached equilibrium [61].

3.2.4. *Adsorption selectivity*

The adsorption selectivity towards certain metal ions within an aqueous mixture under competitive conditions is

Table 1
Adsorption selectivity of OCMCS-SB for Cd(II) in binary ions systems

Binary system	Metal ions	Adsorption capacity (mmol/g)	Selectivity coefficients
Cd^{2+} - Pb^{2+}	Cd^{2+}	0.38	∞
	Pb^{2+}	0.00	
Cd^{2+} - Zn^{2+}	Cd^{2+}	0.39	∞
	Zn^{2+}	0.00	
Cd^{2+} - Ni^{2+}	Cd^{2+}	0.35	8.75
	Ni^{2+}	0.04	

Temperature: 25°C, initial concentration: 2 mmol/L, adsorbent dose: 20 mg

very important. The adsorption selectivity of OCMCS-SB for metal ions was investigated in binary component systems (Table 1). The Cd(II) was prior to be adsorbed by OCMCS-SB in the coexistence of Cd^{2+} - Pb^{2+}, Cd^{2+} - Ni^{2+}, Cd^{2+} - Zn^{2+}. OCMCS-SB has excellent adsorption selectivity for Cd(II), therefore, capable of removing Cd(II) from the multi-ionic system.

3.2.5. Adsorption isotherms

Adsorption isotherm was carried out by varying initial concentrations of Cd(II) from 20 to 200 mg/L at 30°C, with pH at 5.5. It shows the experiments at different initial Cd(II) concentration in Fig. 9. Obviously, the retort of Cd(II) increased sharply in the first stage as the initial concentration raised until the stable point was attained a platform beyond 140 mg/L, and then reached the saturation.

Adsorption isotherms usually fit the Langmuir model and the Freundlich model. The Langmuir Eq. (2) used here can be expressed as [62]:

$$\frac{C_e}{Q_e} = \frac{C_e}{Q_{\max}} + \frac{1}{Q_{\max} K_L} \tag{2}$$

where $Q_{\max}$ (mg/g) is the saturated adsorption capacity and K_L (L/mg) are Langmuir constants. The Langmuir isotherm fitting line (Fig. S1) and the relevant parameters are listed in Table 2. The correlation coefficient (R^2) is near to one and the saturated adsorption capacity ($Q_{\max}$) calculated from the Langmuir model is near to the experimentally gained adsorption capacity ($Q_{e,\exp}$). It can be concluded that the adsorption of Cd(II) on OCMCS-SB fits well with the Langmuir adsorption isotherm.

The dimensionless separation factor (R_L) is calculated by the following Eq. (3) [63]:

$$R_L = \frac{1}{1 + C_0 K_L} \tag{3}$$

where C_0 stands for the highest initial Cd(II) concentration. The R_L values shown in Table 2 (0.165) at concentrations 16–200 mg/L for Cd(II), implies that the adsorption is favorable ($0 < R_L < 1$) [64,65], therefore OCMCS-SB is an appropriate adsorbent for Cd(II) removal.

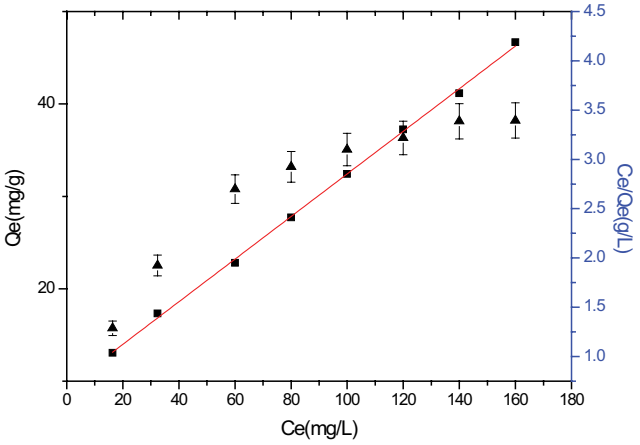

Fig. 9. Effect of initial concentration on adsorption capacity of Cd(II) (▲), and Langmuir adsorption model (■).

The mathematical form of Freundlich isotherm Eq. (4) is [66]:

$$\ln Q_e = \ln K_F + \frac{1}{n} \ln C_e \tag{4}$$

In which K_F (mmol/g) is the Freundlich constants; n is adsorption intensity exponent (dimensionless); Q_e is defined as in equilibrium (mg/g). The adsorption isotherm parameters calculated from the two models are summarized in Table 2. The plot of $\ln Q_e$ vs. $\ln C_e$ gives a relatively lower correlation coefficient (R^2 = 0.98) (Fig. S2) than Langmuir adsorption isotherm, indicating that the adsorption of Cd(II) on OCMCS-SB fits Langmuir model better than Freundlich model. Moreover, the maximum adsorption capacities calculated from the Langmuir model are more consistent with the experimental results which further suggesting the Langmuir model is more suitable for elaborating the isotherm data.

The equilibrium data were also treated by the Dubinin–Radushkevich (D–R) isotherm model conform to the adsorption process is physical or chemical. If the E value shows between 8 and 16 kJ/mol, the adsorption is chemically [66,67]. The calculated E values are 14.2 kJ/mol, suggesting the uptake of Cd(II) was performed in chemisorption.

It gives the adsorption capacities of OCMCS-SB compared with some results from literature for the adsorptions of Cd(II) ion (Table 3). The OCMCS-SB has a relatively adsorption capacity of 46.72 mg/g for Cd(II), illustrating that OCMCS-SB can be a useful material in comparison with existing adsorbents for metal ions treatment from aqueous solutions.

Wang et al. [39] reported a value of 262.47 mg/g with Langmuir isotherm model, and within this work, we are reporting a value of 46.72 mg/g with the same model, the situation is different, [39] the chitosan derived material was made upon the reaction between sodium alginate which is a commercial polysaccharide material and the chitosan derived Schiff base, therefore, this material can be regarded as two polymeric chains joined by a glycerol moiety, as expected the hydroxyl groups of the two polysaccharides

Table 2
Constants and correlation coefficients of adsorption isotherms for adsorption Cd(II) on OCMCS-SB

Adsorbent	Isotherm model							
		Langmuir			Freundlich			
	Q_{max} (mg/g)	K_L (L/mg)	R_L	R^2	n	$1/n$	K((mg/g/mg)$^{1/n}$)	R^2
OCMCS-SB	46.72	0.03	0.165	0.9989	2.33	0.4284	19.05	0.9801

Table 3
Comparison of maximum adsorption capacities of Cd(II) on various adsorbents

Adsorbent	Adsorption capacity (mg/g)	References
Schiff base@Fe_3O_4 composites	89.92	[18]
Cross-linked thiocarbohydrazide-chitosan gel	137.3	[30]
ECH cross-linked chitosan Schiff base-sodium alginate	262.47	[39]
Modified cellulose	279.33	[56]
Nanofibrillar chitosan	60.86	[68]
OCMCS-SB	46.72	This work

Table 4
Kinetic parameters for adsorption of Cd(II) on OCMCS-SB

	Pseudo-first-order kinetics			Pseudo-second-order kinetics		
$Q_{e,exp}$(mg/g)	$Q_{e,cal}$(mg/g)	k_1 (min^{-1})	R_1^2	$Q_{e,cal}$(mg/g)	k_2 (g/mg/min)	R_2^2
44.78	42.52	–0.00842	0.9804	48.47	3.43×10^{-4}	0.9903

and the consequent supramolecular and porous arrangement of the material is reflected on the high capacity to absorb heavy metal ions both, physically (ions trapped within the material) and chemically (ions complexed with hydroxyl groups). In the present study, the structure has been modified and in the absence of the alginate and the replacement with the O-carboxymethyl group, an interesting proposal emerges because, in the absence of the alginate the absorption of cadmium can be attributed completely to a complexation process with the chitosan-modified material, the O-carboxymethyl moiety with the Schiff base provides of two ligands within the same structure, both capable of absorption of cadmium, of course, the absorbing capacity is a little bit lower in comparison from the material [39], nevertheless since the absorption is attributed mainly to chemisorption it represents an improvement since the last communication, thus an emerging material with enhanced properties is proposed and the corresponding complexation chemistry will be further studied.

3.2.6. Adsorption kinetics

To examine the kinetics mechanism which commands the adsorption process, the pseudo-first-order and pseudo-second-order models were used to evaluate the experimental data.

The pseudo-first-order Eq. (5) and the pseudo-second-order (6) is expressed as [19]:

$$\ln\left(Q_e - Q_t\right) = \ln Q_e - k_1 t \tag{5}$$

$$\frac{t}{Q_t} = \frac{1}{k_2 Q_e^2} + \frac{t}{Q_e} \tag{6}$$

where Q_t (mg/g) is the amount of Cd(II) adsorbed by the adsorbent at time t (min), t is the adsorption time, k_1 (1/min) and k_2 (g/mg/min) are the rate constants for pseudo-first-order and the pseudo-second-order models, respectively.

All the related parameters are present in Table 4. The pseudo-second-order has high correlation coefficients and the calculated Q_e also near to the experimental data. Therefore, the rates of adsorption are following the pseudo-second-order model.

3.2.7. Adsorption thermodynamics

The dependence of the adsorption capacity of Cd(II) with temperature as shown in Fig. 10. The adsorption capacity of Cd(II) using OCMCS-SB rises as temperature increases, indicating that the adsorption reaction is endothermic.

The adsorption thermodynamics parameters were calculated by Eqs. (7) and (8) [69]:

$$\ln K_L = \frac{\Delta S^\circ}{R} - \frac{\Delta H^\circ}{RT} \tag{7}$$

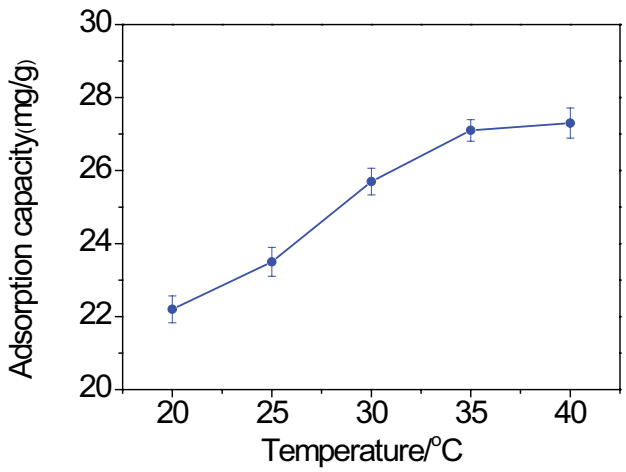

Fig. 10. Effect of temperature on adsorption capacity of Cd(II).

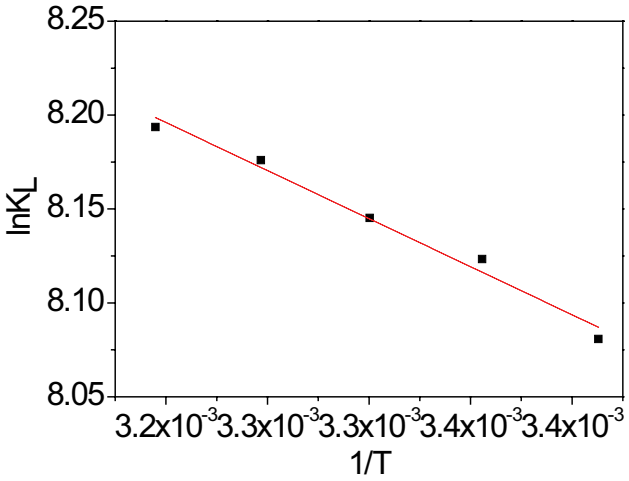

Fig. 11. Thermodynamics plots on adsorption of Cd(II).

$$\Delta G^\circ = -RT\ln K_L \tag{8}$$

where R (8.314 J/mol K) is the ideal gas constant, T (K) is the temperature and K_L (mL/mmol) delegates Langmuir constant, ΔG° is the Gibbs free energy change, ΔS° is the entropy change, and ΔH° is the enthalpy of the adsorption process. Fig. 11 shows the plot of $\ln K_L$ vs. $1/T$ according to Eq. (7). As shown in Table 5, the values of ΔG° are negative, which indicates Cd(II) is adsorbed by OCMCS-SB spontaneously. Additionally, the values of ΔG° became more negative with increasing temperature, hence, the spontaneity of the Cd(II) adsorption increases with the temperature.

Table 5
Thermodynamics parameters for Cd(II) on OCMCS-SB

Adsorbent	ΔS° (J/mol/K)	ΔH° (kJ/mol)	T(K)	ΔG° (kJ/mol)
OCMCS-SB	81.75	4.26	293	–19.68
			298	–20.13
			303	–20.55
			308	–20.94
			313	–21.32

3.3. Recycle and recovery analysis

Regeneration and reuse of adsorbents are highly desirable within the context of green chemistry and related fields. The recovery and recycle experiments are shown in Fig 12. In this study solutions of HCl (pH 1.0) and EDTA were used as desorption media for Cd (II). It can be seen that the adsorption capacity of OCMCS-SB decreased slightly with the increase of the cycles. However, the loaded amount of Cd(II) by regenerated OCMCS-SB after five cycles was 91.58% of the amount by the fresh adsorbent, which proves that OCMCS-SB could be applied in the field of heavy metal ions adsorption.

The desorption of Cd(II) was found to be 96.81% in HCl. At this pH, condition desorption takes place due to the protonation of acid sites on the adsorbent. For desorption carried out by EDTA solution, the desorption of Cd(II) on from OCMCS-SB reaches up to 98.21% after the first cycle. This could be attributed to the different mechanisms of the reagents. EDTA can form a steady complex with metal ions. However, desorption took place in the HCl solution mainly due to the ion exchange. The desorbed OCMCS-SB was highly effective for the re-adsorption of Cd(II), and the adsorption ability of OCMCS-SB was kept constant after several repetitions of the adsorption–desorption cycles.

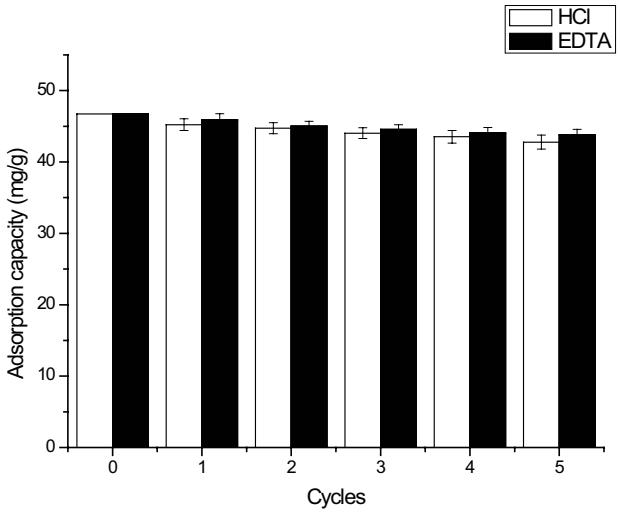

Fig. 12. Adsorption capacity of Cd(II) on OCMCS-SB in five cycles with different desorptions.

3.4. Adsorption mechanism

The adsorption mechanism for Cd(II) had been discussed elsewhere, such as the Cd (II) adsorption with thiocarbohydrazide-chitosan was dominated by coordination process [29]. The –OH, N–H and C=N groups took part in

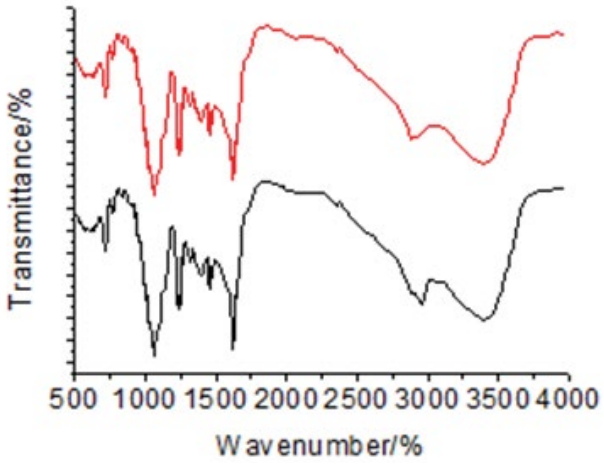

Fig. 13. IR of OCMCS-SB fresh (up) and after (down) adsorption.

the adsorption of the Cd(II) ions and amine groups interacted with the Cd(II) ions as well. Thus the O, N atoms contributed to the formation of Cd(II)-related coordination complexes. Additionally, the lone pairs of electrons in the O, N atoms possibly shared the bond with Cd(II), and this resulted in the electron cloud density of atom decreasing and the binding energy increases [30]. Since $Cd(CH_3COO)_2$ was used, there is no significant difference between recycling and fresh OCMCS-SB (Fig. 13). Besides, considering the desorption with EDTA, we speculated that the Cd(II) adsorption process was mainly dominated by a coordination reaction process.

4. Conclusions

With carboxymethylation of chitosan, a novel Schiff base was successfully synthesized from OCMCS and o-vanillin. The resulting compounds were characterized by FTIR, thermogravimetric analysis/differential thermal gravity (TG/DTG), XRD, and SEM. It was found that the crystallinity of the synthesized OCMCS-SB was lower than that of chitosan, but the thermal stability was more stable than that of chitosan. Adsorption experiment of Cd(II) has been used to test OCMCS-SB as an adsorbing material. The best pH value of adsorption of Cd(II) is 5.5, while the maximum adsorption capacity is 46.72 mg/g. The adsorption isotherms of Cd(II) are best described by the Langmuir model. The kinetic data demonstrated to be suited to a pseudo-second-order model. The loaded amount of Cd(II) by regenerated OCMCS-SB after five cycles was 91.58% of the amount by the fresh adsorbent, which proves that OCMCS-SB could be applied in the field of heavy metal ions adsorption.

Acknowledgment

This work was supported by the Ph.D. Programs Foundation of Ludong University (No. 32840301), and the National University Student Innovation and entrepreneurship training Program (201810451326, 201810451344).

References

[1] G. Zong, H. Chen, R. Qu, C. Wang, N. Ji, Synthesis of polyacrylonitrile-grafted cross-linked N-chlorosulfonamidated polystyrene via surface-initiated ARGET ATRP, and use of the resin in mercury removal after modification, J. Hazard. Mater., 186 (2011) 614–621.
[2] D.K. Singh, S. Mishra, Synthesis, characterization, and removal of Cd(II) using Cd(II)-ion imprinted polymer, J. Hazard. Mater., 164 (2009) 1547–1551.
[3] C.V. Gherasim, G. Bourceanu, R.I. Olariu, A novel polymer inclusion membrane applied in chromium (VI) separation from aqueous solutions, J. Hazard. Mater., 197 (2011) 244–253.
[4] M.M. Matlock, B.S. Howerton, D.A. Atwood, Chemical precipitation of heavy metals from acid mine drainage, Water Res., 36 (2002) 4757–4764.
[5] L. Zhang, Y.H. Zhao, R. Bai, Development of a multifunctional membrane for chromatic warning and enhanced adsorptive removal of heavy metal ions: application to cadmium, J. Membr. Sci., 379 (2011) 69–79.
[6] C. Zhang, M. Jin, C. Sun, R. Qu, Y. Zhang, Synthesis of polyamine-bridged polysilsesquioxanes and their adsorption properties for heavy metal ions, Environ. Prog. Sustainable Energy, 36 (2017) 1089–1099.
[7] C. Liu, X. Sun, L. Liu, J. Liu, M. Qi, H. An, Synthesis of 8-hydroxyquinoline-functionalized polyglycidy methacrylate resin and its efficient adsorption and desorption for Pb(II), Desal. Water Treat., 57 (2016) 18425–18437.
[8] Y. Niu, R. Qu, C. Sun, C. Wang, H. Chen, C. Ji, Y. Zhang, X. Shao, F. Bu, Adsorption of Pb(II) from aqueous solution by silica-gel supported hyperbranched polyamidoamine dendrimers, J. Hazard. Mater., 244–245 (2013) 276–286.
[9] X. Song, Y. Niu, P. Zhang, C. Zhang, Z. Zhang, Y. Zhu, R. Qu, Removal of Co(II) from fuel ethanol by silica-gel supported PAMAM dendrimers: combined experimental and theoretical study, Fuel, 199 (2017) 91–101.
[10] L. Guo, C. Sun, G. Li, C. Liu, C. Sun, Thermodynamics and kinetics of Zn(II) adsorption on cross-linked starch phosphates, J. Hazard. Mater., 161 (2009) 510–515.
[11] Y. Niu, H. Liu, R. Qu, S. Liang, H. Chen, C. Sun, Y. Cui, Preparation and characterization of thiourea-containing silica gel hybrid materials for Hg(II) adsorption, Ind. Eng. Chem. Res., 54 (2015) 1656–1664.
[12] C. Sun, G. Zhang, C. Wang, R. Qu, Y. Zhang, Q. Gu, A resin with high adsorption selectivity for Au (III): preparation, characterization and adsorption properties, Chem. Eng. J., 172 (2011) 713–720.
[13] F. Cao, P. Yin, X. Liu, C. Liu, R. Qu, Mercury adsorption from fuel ethanol onto phosphonated silica gel prepared by heterogenous method, Renewable Energy, 71 (2014) 61–68.
[14] C. Dong, R. Fu, C. Sun, R. Qu, C. Ji, Y. Niu, Y. Zhang, Comparison studies of adsorption properties for copper ions in fuel ethanol and aqueous solution using silica-gel functionalized with 3-amino-1,2-propanediol, Fuel, 226 (2018) 331–337.
[15] X. Song, Y. Niu, Z. Qiu, Z. Zhang, Y. Zhou, J. Zhao, H. Chen, Adsorption of Hg(II) and Ag(I) from fuel ethanol by silica gel supported sulfur-containing PAMAM dendrimers: kinetics, equilibrium, and thermodynamics, Fuel, 206 (2017) 80–88.
[16] Y. Zhang, R. Qu, C. Sun, C. Sun, H Chen, P. Yin, Improved synthesis of a silica-gel-based dendrimer-like highly branched polymer as the Au(III) adsorbent, Chem. Eng. J., 270 (2015) 110–121.
[17] S. Zhang, Y. Zhang, J. Liu, Q. Xu, H. Xiao, X. Wang, H. Xu, J. Zhou, Thiol modified Fe_3O_4@SiO_2 as a robust, high effective, and recycling magnetic sorbent for mercury removal, Chem. Eng. J., 226 (2013) 30–38.
[18] J. Zhao, Y. Niu, B. Ren, H. Chen, S. Zhang, J. Jin, Y. Zhang, Synthesis of Schiff base functionalized superparamagnetic Fe_3O_4 composites for effective removal of Pb(II) and Cd(II) from aqueous solution, Chem. Eng. J., 347 (2018) 574–584.
[19] Y. Wang, R. Qu, F. Pan, X. Jia, C. Sun, C. Ji, Y. Zhang, K. An, Y. Mu, Preparation and characterization of thiol- and amino-functionalized polysilsesquioxane coated

poly(p-phenylenetherephthal amide) fibers and their adsorption properties towards Hg(II), Chem. Eng. J., 317 (2017) 187–203.
[20] P. Yin, Q. Xu, R. Qu, G. Zhao, Y. Sun, Adsorption of transition metal ions from aqueous solutions onto a novel silica gel matrix inorganic–organic composite material, J. Hazard. Mater., 173 (2010) 710–716.
[21] D. Wang, Y. Xu, D. Xiao, Q. Qiao, P. Yin, Z. Yang, J. Li, W. Winchester, Z. Wang, T. Hayat, Ultra-thin iron phosphate nanosheets for high efficient U(VI) adsorption, J. Hazard. Mater., 371 (2019) 83–93.
[22] S. Zhang, Y. Zhang, G. Bi, J. Liu, Z. Wang, Q. Xu, H. Xu, X. Li, Mussel-inspired polydopamine biopolymer decorated with magnetic nanoparticles for multiple pollutants removal, J. Hazard. Mater., 270 (2014) 27–34.
[23] R. Li, J.J. Wang, L.A. Gaston, B. Zhou, M. Li, R. Xiao, Q. Wang, Z. Zhang, H. Huang, W. Liang, H. Huang, X. Zhang, An overview of carbothermal synthesis of metal–biochar composites for the removal of oxyanion contaminants from aqueous solution, Carbon, 129 (2018) 674–687.
[24] M. Xu, P. Yin, X. Liu, X. Dong, Y. Yang, Z. Wang, R. Qu, Optimization of biosorption parameters of Hg(II) from aqueous solutions by the buckwheat hulls using respond surface methodology, Desal. Water Treat., 51 (2013) 4546–4555.
[25] L. Wei, P. Yin, Z. Yang, Y. Xu, W. Jiang, J. Jin, H. Cai, Z. Guo, Enhanced uptake of gold ions from wastewater due to covalent functionalization of organotriphosphonic acid on japonica shells, Desal. Water Treat., 139 (2019) 228–245.
[26] C. Liu, Yongrui Pi, G. Ju, Z. Wang, Adsorptive removal of Cu^{2+} and direct sky blue 5B from aqueous by acid-treated tea waste—application of response surface methodology, Desal. Water Treat., 143 (2019) 256–267.
[27] M. Mahlous, D. Tahtat, S. Benamer, Gamma irradiation-aided chitin/chitosan extraction from prawn shells, Nucl. Instrum. Methods Phys. Res., Sect. B, 265 (2007) 414–417.
[28] G. Li, Y. Meng, L. Guo, T. Zhang, J. Liu, Formation of thermo-sensitive polyelectrolyte complex micelles from two biocompatible graft copolymers for drug delivery, J. Biomed. Mater. Res. Part A, 102 (2014) 2163–2172.
[29] R. Li, Wen. Liang, M. Li, S. Jiang, H. Huang, Z. Zhang, J.J. Wang, M.K. Awasthi, Removal of Cd(II) and Cr(VI) ions by highly cross-linked thiocarbohydrazide-chitosan gel, Int. J. Biol. Macromol., 104 (2017) 1072–1081.
[30] R. Li, W. Liang, H. Huang, S. Jiang, D. Guo, M. Li, Z. Zhang, A. Ali, J.J. Wang, Removal of cadmium(II) cations from an aqueous solution with aminothiourea chitosan strengthened magnetic biochar, J. Appl. Polym. Sci., 135 (2018) 46239.
[31] M. Qi, G. Li, N. Yu, Y. Meng, X. Liu, Synthesis of thermo-sensitive polyelectrolyte complex nanoparticles from CS-g-PNIPAM and SA-g-PNIPAM for controlled drug release, Macromol. Res., 22 (2014) 1004–1011.
[32] G. Li, L. Guo, Y. Meng, T. Zhang, Self-assembled nanoparticles from thermo-sensitive polyion complex micelles for controlled drug release, Chem. Eng. J., 174 (2011) 199–205.
[33] G. Li, Q. Wen, T. Zhang, Y. Ju, Synthesis, and properties of silver nanoparticles in chitosan-based thermo-sensitive semi-interpenetrating hydrogels, J. Appl. Polym. Sci., 127 (2013) 2690–2697.
[34] R. Qu, C. Sun, M. Wang, C. Ji, Q. Xu, Y. Zhang, C. Wang, H. Chen, P. Yin, Adsorption of Au(III) from aqueous solution using a cotton fiber/chitosan composite adsorbents, Hydrometallurgy, 100 (2009) 65–71.
[35] M. Wang, R. Qu, C. Sun, Y. Niu, Y. Zhang, J. Gao, H. Cai, X. Song, Synthesis, characterization, and adsorption properties of m-aramid and chitosan hybrid composite films with the ratio of 100/0, 85/15, 65/35, 50/50 and 35/65 toward Hg(II) ions, Desal. Water Treat., 146 (2019) 197–209.
[36] F. Ma, R. Qu, C. Sun, C. Wang, C. Ji, Y. Zhang, P. Yin, Adsorption behaviors of Hg(II) on chitosan functionalized by amino-terminated hyperbranched polyamidoamine polymers, J. Hazard. Mater., 172 (2009) 792–801.
[37] R. Qu, C. Sun, F. Ma, Y. Zhang, C. Ji, Q. Xu, C. Wang, H. Chen, Removal and recovery of Hg(II) from aqueous solution using chitosan-coated cotton fibers, J. Hazard. Mater., 167 (2009) 717–727.
[38] W. Wang, Q. Lu, X. Ren, C. Liu, J. Jin, S. Yin, J. Zhang, J. Zhou, Synthesis of novel ECH cross-linked chitosan Schiff base-Sodium alginate for adsorption of Cd(II) ion from aqueous solution, Desal. Water Treat., 145 (2019) 169–178.
[39] W. Wang, R. Poli, D. Agustin, Influence of ligand substitution on molybdenum catalysts with tridentate Schiff base ligands for the organic solvent-free oxidation of limonene using aqueous TBHP as oxidant, Mol. Catal., 443 (2017) 52–59.
[40] W. Wang, J.-C. Daran, R. Poli, D. Agustin, OH-Substituted tridentate ONO Schiff base ligands and related molybdenum(VI) complexes for solvent-free (ep)oxidation catalysis with TBHP as oxidant, J. Mol. Catal. A: Chem., 416 (2016) 117–126.
[41] W. Wang, T. Vanderbeeken, D. Agustin, R. Poli, Tridentate ONS vs. ONO salicylideneamino(thio)phenolato [MoO_2L] complexes for catalytic solvent-free epoxidation with aqueous TBHP, Catal. Commun., 63 (2015) 26–30.
[42] W. Wang, T. Guerrero, S.R. Merecias, H. García-Ortega, R. Santillan, J.-C. Daran, N. Farfán, D. Agustin, R Poli, Substituent effects on solvent-free epoxidation catalyzed by dioxomolybdenum(VI) complexes supported by ONO Schiff base ligands, Inorg. Chim. Acta, 431 (2015) 176–183.
[43] M. Rinaudo, Chitin and chitosan: properties and applications, Prog. Polym. Sci., 31 (2006) 603–632.
[44] B. Zhang, Y. Niu, L. Li, W. Xu, H. Chen, B. Yuan, H. Yang, Combined experimental and DFT study on the adsorption of Co(II) and Zn(II) from fuel ethanol by Schiff base decorated magnetic Fe_3O_4 composites, Microchem. J., 151 (2019) 104220.
[45] Y. Niu, R. Qu, H. Chen, L. Mu, X. Liu, T. Wang, Y. Zhang, C. Sun, Synthesis of silica gel supported salicylaldehyde modified PAMAM dendrimers for the effective removal of Hg(II) from aqueous solution, J. Hazard. Mater., 278 (2014) 267–278.
[46] X.G. Chen, H.J. Park, Chemical characteristics of O-carboxymethyl chitosans related to the preparation conditions, Carbohydr. Polym., 53 (2003) 355–359.
[47] C. Ji, S. Song, C. Wang, C. Sun, R. Qu, C. Wang, H. Chen, Preparation and adsorption properties of chelating resins containing 3-aminopyridine and hydrophilic spacer arm for Hg(II), Chem. Eng. J., 165 (2010) 573–580.
[48] M. Zheng, B. Han, Y. Yang, Synthesis, characterization and biological safety of O-carboxymethyl chitosan used to treat Sarcoma 180 tumor, Carbohydr. Polym., 86 (2011) 231–238.
[49] H.C. Ge, D.K. Luo, Preparation of carboxymethyl chitosan in aqueous solution under microwave irradiation, Carbohydr. Res., 340 (2005) 1351–1356.
[50] T. Sun, W. Xie, P. Xu, Superoxide anion scavenging activity of graft chitosan derivatives, Carbohydr. Polym., 58 (2004) 379–382.
[51] C. Xu, J. Wang, T. Yang, X. Chen, X. Liu, X. Ding, Adsorption of uranium by amidoximated chitosan-grafted polyacrylonitrile, using response surface methodology, Carbohydr. Polym., 121 (2015) 79–85.
[52] X. Liu, H. Chen, C. Wang, R. Qu, C. Ji, C. Sun, Y. Zhang, Synthesis of porous acrylonitrile/methyl acrylate copolymer beads by suspended emulsion polymerization and their adsorption properties after amidoximation, J. Hazard. Mater., 175 (2010) 1014–1021.
[53] C. Sun, R. Qu, S. Song, H. Chen, X. Liu, C. Sun, G. Liu, Synthesis of 2-phenoxyethanol/formaldehyde copolymer beads by dispersion polycondensation and their adsorption properties for copper ions after polyamine modification, Desal. Water Treat., 57 (2016) 13722–13732.
[54] B. Yuan, L. Qiu, H. Su, C. Cao, J. Jiang, Schiff base - Chitosan grafted L-monoguluronic acid as a novel solid-phase adsorbent for removal of congo red, Int. J. Biol. Macromol., 82 (2016) 355–360.
[55] Y. Zhou, X. Hu, M. Zhang, X. Zhuo, J. Niu, Preparation and characterization of modified cellulose for adsorption of Cd(II), Hg(II), and acid fuchsin from aqueous solutions, Ind. Eng. Chem. Res., 52 (2013) 876–84.

[56] A.L. Bacarella, E. Grunwald, H.P. Marshall, E.L. Purlee, The potentiometric measurement of acid dissociation constants and pH in the system methanol-water. pKa values for carboxylic acides and anilinium ions, J. Org. Chem., 20 (1955) 747–762.
[57] R. Díaz-Sobac, A. Vázquez-Luna, E. Rivadeneyra-Domínguez, J.F. Rodríguez-Landa, T. Guerrero, J.S. Durand-Niconoff, New paths of cyanogenesis from enzymatic-promoted cleavage of β-cyanoglucosides are suggested by a mixed DFT/QTAIM approach, J. Mol. Model., 25 (2019) 295.
[58] M. Ciaccia, S. Di Stefano, Mechanisms of imine exchange reactions in organic solvents, Org. Biomol. Chem., 13 (2015) 646–654.
[59] E.L. Blinn, D.H. Busch, Reactions of coordinated ligands. XV. Demonstration of the kinetic coordination template effect, Inorg. Chem., 7 (1968), 820–824.
[60] J.G. Martins, M.T. Barros, R.M. Pinto, H.M.V.M. Soares, Cadmium(II), lead(II), and zinc(II) ions coordination of N,N′-(S,S)Bis[1-carboxy-2-(imidazol-4yl)ethyl]ethylenediamine: equilibrium and structural studies, J. Chem. Eng. Data, 56 (2011) 398–405.
[61] R. Qu, Y. Zhang, W. Qu, C. Sun, J. Chen, Y. Ping, H. Chen, Y. Niu, Mercury adsorption by sulfur- and amidoxime-containing bifunctional silica gel-based hybrid materials, Chem. Eng. J., 219 (2013) 51–61.
[62] J. Chen, R. Qu, Y. Zhang, C. Sun, C. Wang, C. Ji, P. Yin, H. Chen, Y. Niu, Preparation of silica gel supported amidoxime adsorbents for selective adsorption of Hg(II) from aqueous solution, Chem. Eng. J., 209 (2012) 235–244.
[63] S. Abbasizadeh, A.R. Keshtkar, M.A. Mousavian, Sorption of heavy metal ions from aqueous solution by a novel cast PVA/TiO_2 nanohybrid adsorbent functionalized with amine groups, J. Ind. Eng. Chem., 20 (2014) 1656–1664.
[64] M. Bozorgi, S. Abbasizadeh, F. Samani, S.E. Mousavi, Performance of synthesized cast and electrospun PVA/chitosan/ZnO-NH_2 nano-adsorbents in single and simultaneous adsorption of cadmium and nickel ions from wastewater, Environ. Sci. Pollut. Res., 25 (2018) 17457–17472.
[65] M. Shafiee, M.A. Abedi, S. Abbasizadeh, R.K. Sheshdeh, S.E. Mousavi, S. Shohani, Effect of zeolite hydroxyl active site distribution on adsorption of Pb(II) and Ni(II) pollutants from water system by polymeric nanofibers, Sep. Sci. Technol., 6 (2019) 1–18.
[66] R. Qu, C. Sun, F. Ma, Z. Cui, Y. Zhang, X. Sun, C. Ji, C. Wang, P. Yin, Adsorption kinetics and equilibrium of copper from ethanol fuel on silica-gel functionalized with amino-terminated dendrimer-like polyamidoamine polymers, Fuel, 92 (2012) 204–210.
[67] Z. Zhang, Y. Niu, H. Chen, Z. Yang, L. Bai, Z. Xue, H. Yang, Feasible one-pot sequential synthesis of aminopyridine functionalized magnetic Fe_3O_4 hybrids for robust capture of aqueous Hg(II) and Ag(I), ACS Sustainable Chem. Eng., 7 (2019) 7324–7337.
[68] D. Liu, Z. Li, Y. Zhu, Recycled chitosan nanofibril as an effective Cu(II), Pb(II) and Cd(II) ionic chelating agent: adsorption and desorption performance, Carbohydr. Polym., 111 (2014) 469–476.
[69] Y.Z. Niu, J.Y. Yang, R.J. Qu, Y.H. Gao, N. Du, H. Chen, C. Sun, W. Wang, Synthesis of silica-gel-supported sulfur-capped PAMAM dendrimers for efficient Hg(II) adsorption: experimental and DFT Study, Ind. Eng. Chem. Res., 55 (2016) 3679–88.

Supporting information

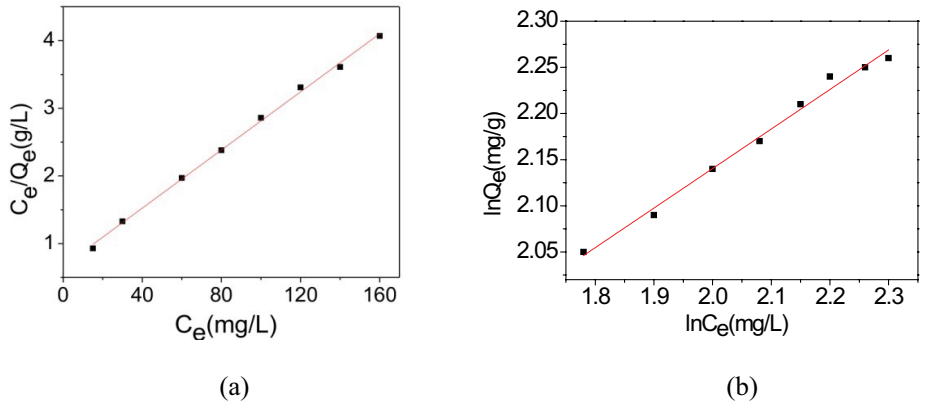

Fig. S1. (a) Langmuir and (b) Freundlich models for adsorption of Cd(II).

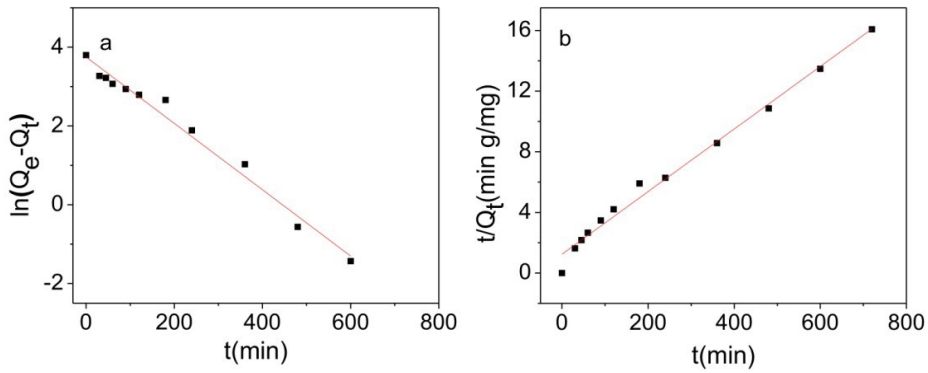

Fig. S2. (a) Pseudo-first-order and (b) pseudo-second-order models for the adsorption of Cd(II).